

Structures, Energetics, and Vibrational Spectra of $\text{H}_2\text{O}_2\cdots(\text{H}_2\text{O})_n$, $n = 1-6$ Clusters: Ab Initio Quantum Chemical Investigations

Anant D. Kulkarni,^{*,†} Rajeev K. Pathak,^{*,‡} and Libero J. Bartolotti[§]

Department of Chemistry, University of Pune, Pune-411 007 India, Department of Physics, University of Pune, Pune-411 007 India, The Abdus Salam International Center for Theoretical Physics, Strada Costiera 11, I-34014, Trieste, Italy, and The Department of Chemistry, East Carolina University, Science and Technology Building, Suite 300, Greenville, North Carolina 27858-4353

Received: December 1, 2004; In Final Form: March 18, 2005

Hydrogen-bonded heteroclusters of $\text{H}_2\text{O}_2\cdots(\text{H}_2\text{O})_n$, with n varying from 1 through 6, have been investigated herein employing ab initio quantum chemical methods. For a given n , several energetically comparable conformers emerge as local minima on the potential energy surface (PES). All of the conformers obtained at restricted Hartree–Fock (RHF) and Møller–Plesset second-order perturbation (MP2) levels of theory exhibit parallel trends in energy hierarchy. The effect of clustering by water on the modification in the vibrational frequencies has also been investigated and further, a many-body interaction-energy analysis is carried out providing insights into cooperativity in $\text{H}_2\text{O}_2\cdots(\text{H}_2\text{O})_n$ clusters.

I. Introduction

Hydrogen Peroxide, H_2O_2 , present in the earth's atmosphere in traces (on an average, ~ 4 ppb¹), is a substance that plays an important role in diversified phenomena.^{1–7} H_2O_2 is a dominant oxidant in clouds, fog, and rain, effecting the aqueous oxidation of SO_2 ; it is a powerful disinfectant, a useful chemical inside and outside the human body,⁸ a catalyst for several inorganic and inorganic reactions, and so forth.^{8,9} Recent literature discusses several chemical reactions involving hydrogen peroxide as one of the reactants.^{9–16} In particular, hydrogen-bonded complexes of H_2O_2 form an important subdomain of hydrogen peroxide chemistry, a subject that has been studied extensively employing experimental and theoretical techniques, as highlighted below.

The mechanism of the first oxidation step of disulfides to thiosulfates by H_2O_2 has been studied theoretically at the RHF/6-31G(d,p) level by Benassi and co-workers.⁹ A series of hydrogen-bonded complexes of H_2O_2 with other species such as $(\text{CH}_3)_2\text{O}$, NH_3 , $\text{N}(\text{CH}_3)_3$, phosphorus, and sulfur bases as well as HX ($X = \text{F}, \text{Cl}, \text{Br}, \text{etc.}$) have been studied by Del Bene and others^{10,11} using matrix isolation. They also corroborated their findings on the theoretical front by ab initio techniques. It should be noted that most of these studies involved computations at a respectable MP2/6-31G(d,p) level, and the results are indeed in good agreement with the vibrational frequencies observed experimentally. Shir and Zhou¹² employed a DFT-based approach to study cyclic hydrogen-bonded complexes between hydrogen peroxide and glycine where H_2O_2 plays a dual role of proton donor as well as acceptor. Ab initio studies focusing on complexes of sulfuric acid with various trace gas species including H_2O_2 were carried out by Beichert and Schremes,¹³ the focus of their work being the stabilities of sulfuric acid

complexes with HCl , H_2O , HNO_3 , and so forth. Further, Dobado and co-workers^{14,15} carried out a series of studies on the hydrogen-bonded systems of hydrogen peroxide with various other molecules. Their investigations demonstrated that H_2O_2 forms stable cyclic hydrogen-bonded structures. They also advocated that the density-functional-theory (DFT)-based methods show good agreement in reproducing the geometrical parameters and energies that are comparable with the corresponding MP2-level as well as experimental counterparts.

A notable theoretical study by Gonzalez et al.¹⁶ compares the calculations for the H_2O_2 dimer and $\text{H}_2\text{O}_2\cdots\text{H}_2\text{O}$ complex at MP2 and DFT for investigation of the interaction energies and O–H frequency shifts in multiple-hydrogen-bonded systems. They observed that in the $\text{H}_2\text{O}_2\cdots\text{H}_2\text{O}$ complex each unit can behave either as a hydrogen-bond donor or acceptor forming cyclic structures that generally involve nonidentical hydrogen bonds. This study demonstrates that density-functional-theory-based methods (DFT) yield energies and vibrational shifts sizably overestimated than those at the MP2 level. More recently, interesting accurate experimental as well as supporting theoretical investigations have been carried out on the peroxide dimer by Engdahl, Nelander, and Karlström.¹⁷ Engdahl et al. performed a low-temperature Ar-matrix isolation as well as an ab initio study of the H_2O_2 dimer and its deuterated analogues and proposed that the dimer at the MP2 level exhibits a “cyclic” structure with two hydrogen bonds, and further confirmed this finding through their experimental IR spectra.

In their careful ab initio analysis of the $\text{H}_2\text{O}_2\cdots\text{H}_2\text{O}$ complex, Dobado and Molina¹⁸ discovered three minima and two transition-state structures for this 1:1 complex. They estimated the binding energy of this heterocluster to be 6.4 ± 0.2 kcal·mol⁻¹, typical of the hydrogen-bonded complexes. Mo and co-workers¹⁹ carried out investigations of the structures, vibrational frequencies, and thermodynamic properties of $\text{H}_2\text{O}_2\cdots\text{H}_2\text{O}$ complexes. According to this work, the global minimum at the Hartree–Fock (HF) and MP2 levels is a “five-membered” (comprising the covalent and H bonds together) $\text{H}_2\text{O}_2\cdots\text{H}_2\text{O}$ complex showing a red shift due to OH stretching.

* Corresponding authors. E-mail: anantkul@yahoo.com (A.D.K.); pathak@physics.unipune.ernet.in (R.K.P.).

[†] Department of Chemistry, University of Pune.

[‡] Department of Physics, University of Pune and the Abdus Salam International Center for Theoretical Physics.

[§] East Carolina University.

Recently, Kulkarni et al.^{20a} have explored hydrogen peroxide clusters (H_2O_2)_n, $n = 2-4$, using ab initio techniques. This study at the MP2 level shows the ability of H_2O_2 to form a 3D network similar to the corresponding water clusters. This is borne out from the structures of the H_2O_2 dimer, trimer, and tetramer reported in this study exhibiting a remarkable similarity to the respective H_2O -cluster structural patterns. Interestingly, the mixture of H_2O_2 and H_2O is known to be explosive in nature, whereas H_2O_2 decomposes into H_2O and O_2 when heated at 80 °C. The structures as well as thermodynamic properties of $\text{H}_2\text{O}_2 \cdots (\text{H}_2\text{O})_n$, $n = 1-3$, complexes have been reported recently by Ju and others.²¹

All of the aforementioned works discuss $\text{H}_2\text{O}_2 \cdots (\text{H}_2\text{O})_n$ systems up to $n = 3$. The present article embodies inferences drawn from a comprehensive investigation on H_2O_2 with additional water molecules attached. Herein, we study $\text{H}_2\text{O}_2 \cdots (\text{H}_2\text{O})_n$ for $n = 1-6$ to determine their structures at various levels of theory, augmented by an analysis of the vibrational spectrum of these clusters. It is also aimed at providing, at the molecular level, a tool to unravel the cooperative effects, the basis set effect, and the trends in energetics and structures as well as determining the similarity patterns to $(\text{H}_2\text{O})_n$ clusters.

II. Methodology

The structures of $\text{H}_2\text{O}_2 \cdots (\text{H}_2\text{O})_n$, $n = 1-6$, are generated by the supermolecular approach and from the knowledge of the lowest-energy $(\text{H}_2\text{O}_2)_n$ ^{20a} and $(\text{H}_2\text{O})_n$ clusters.²² These systems were optimized using the GAUSSIAN98²³ and GAMESS suit²⁴ of programs at RHF and MP2 levels. We have employed a decent basis set, 6-31G(d,p) (with 25 and 40 basis functions for the water and H_2O_2 molecule, respectively), as well as an accurate basis set, namely, 6-311++G(2d,2p) with additional 6d and 10f functions (49 and 78 basis functions for the H_2O and H_2O_2 molecules, respectively) to satisfactorily include electron correlation that is crucial for the description of such weakly H-bonded complexes. The basis set employed herein is superior to the one employed in the earlier study by Ju et al.²¹ in which the number of basis functions employed is 41 for water and 64 for the peroxide molecule. In view of the large number of possible geometries for these clusters, one encounters several minima strewn on a shallow potential energy surface, making it extremely arduous to locate the genuine energy minimum for each cluster. Nevertheless, we have scanned around 30 structures for $n = 3-6$, each at the RHF/6-31G(d,p) level, and have chosen the energetically minimal and hence the most favorable structure(s) for the follow-up at a higher level with an improved basis set. Also, we could ascertain that the minimum-energy structures reported in this study indeed correspond to (at least local) minima by computing the vibrational frequencies at the MP2/6-311++G(2d,2p) (6d,10f) level.

The structure generation and visualization and the vibrational frequency analysis have been implemented by employing two user-friendly visualization packages, UNIVIS-2000²⁵ and MOLDEN.²⁶ Many-body interaction-energy analysis and BSSE corrections have been performed using the MBAC program developed by Kulkarni et al.²⁷ The term “many-body” in the present context means pairwise (two-body), three-body, four-body (wherever pertinent), and so forth, interactions among different monomers in the given molecular cluster. The units herein are thus the individual molecules constituting the weakly bonded complex, in the present case, through hydrogen-bonding. The concept we have employed has the same implication as described by Elrod and Saykally,²⁸ Xantheas,^{20b} and more

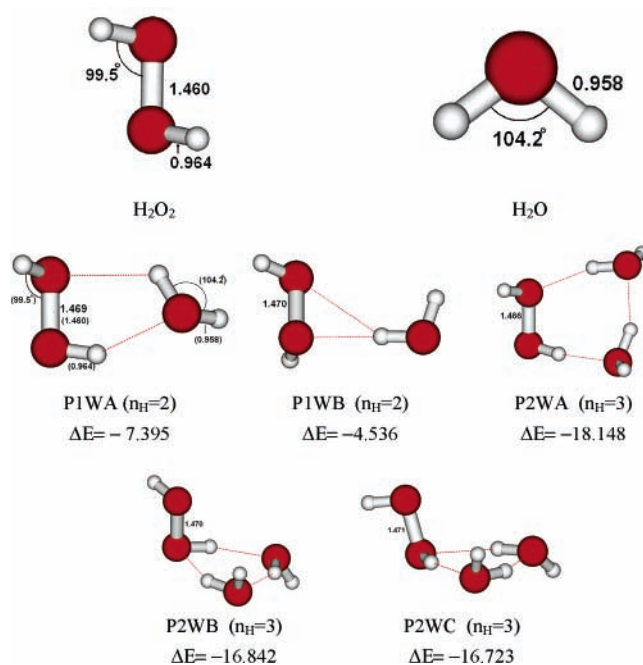


Figure 1. MP2/6-311++G(2d,2p) (6d,10f) optimized structures of $\text{H}_2\text{O}_2 \cdots (\text{H}_2\text{O})_n$, $n = 1-2$ clusters, along with the number of hydrogen bonds (n_{H}), O—O distances, and the corresponding interaction energies in $\text{kcal}\cdot\text{mol}^{-1}$. For structure P1WA, the values in the parentheses correspond to those for the isolated molecules at the same level of theory. All of the distances are given in angstroms. Refer to the text for further details.

recently by Kulkarni et al.²⁷ Also, to gauge the effect of the basis set on BSSE correction, we have performed the sample calculation for typical $\text{H}_2\text{O}_2 \cdots (\text{H}_2\text{O})_n$, $n = 1, 2$ complexes at the MP2/aug-cc-pV5Z//MP2/6-311++G(2d,2p)(6d,10f) level.

Thus, we have performed the computations at three different levels with increasing effect of correlation, under two different basis sets, namely, RHF/6-31G(d,p), MP2/6-31G(d,p), and MP2/6-311++G(2d,2p)(6d,10f). For an accurate estimation of the interaction energies and geometrical parameters, we have employed the most sophisticated of these, namely, MP2/6-311++G(2d,2p) (6d,10f), and the entire discussion on the $\text{H}_2\text{O}_2 \cdots (\text{H}_2\text{O})_n$, $n = 1-6$, cluster systems pertains to this level as presented below.

III. Results and Discussion

Structural Investigation. For the simplest case of $n = 1$, that is, the $\text{H}_2\text{O}_2 \cdots \text{H}_2\text{O}$ system's two lowest-energy structures, labeled P1WA and P1WB, are seen to arise (cf. Figure 1 that also displays the H bonds), with their interaction energies at the MP2/6-311++G(d,2p) (6d,10f) level (used throughout, unless otherwise indicated), respectively, being -7.395 and $-4.536 \text{ kcal}\cdot\text{mol}^{-1}$. Table 1 presents the detailed energetics for all of the structures: interaction energies at different levels and basis sets used herein, along with the zero-point-energy (ZPE)-as well as basis-set superposition-error (BSSE)-corrected interaction energies. The hydrogen-bonded cyclic structure (P1WA) matches well with the previously studied minimum-energy structure by experimental as well as theoretical techniques.^{16,17} For $n = 2$, the three energetically most favorable structures, namely, P2WA, P2WB, and P2WC, emerge, falling within the energy range of $\pm 1.5 \text{ kcal}\cdot\text{mol}^{-1}$ with respect to one another. These structures are also depicted in Figure 1 along with their interaction energies and the three hydrogen bonds they possess. The most stable structure (P2WA) may be viewed as a

TABLE 1: Raw^a, ZPE-Corrected, and BSSE-Corrected Interaction Energies (in kcal·mol⁻¹) of H₂O₂⋯(H₂O)_n, n = 1–6, Clusters at RHF/6-31G(d,p), MP2/6-31G(d,p) and MP2/6-311++G(2d,2p)(6d,10f) Levels

str. code	$\Delta E(\text{RHF/I})^b$	$\Delta E(\text{MP2/I})^c$	$\Delta E(\text{MP2/II})^d$	$\Delta E_{\text{BSSE-corr}}^e$	$\Delta E_{\text{ZPE-corr}}^f$	$\Delta E_{\text{ZPE+BSSE}}^g$
P1WA	-8.468	-11.157	-7.395	-6.397	-5.053	-4.055
P1WB	-5.021	-11.132	-4.536	-3.689	-2.904	-2.057
P2WA	-19.064	-24.561	-18.148	-15.813	-13.152	-10.817
P2WB	-18.198	-24.322	-16.824	-14.614	-12.132	-9.922
P2WC	-17.959	-23.940	-16.723	-14.602	-12.050	-9.929
P3WA	-29.728	-39.514	-29.217	-25.709	-21.798	-18.290
P3WB	-29.157	-38.579	-28.527	-25.126	-21.240	-17.839
P3WC	-29.164	-37.920	-28.464	-25.063	-21.188	-17.787
P3WD	-29.000	-38.247	-28.426		-21.184	
P3WE	-28.950	-37.920	-28.464		-21.180	
P4WA	-38.962	-50.589	-38.717	-34.212	-29.026	-24.521
P4WB	-38.968	-50.589	-38.717	-34.207	-29.026	-24.516
P4WC	-39.025	-51.481	-38.648	-34.058	-28.866	-24.276
P4WD	-39.207	-53.340	-37.882		-28.088	
P4WE ^h	-39.207	-53.338	-37.877		-28.452	
P5WA	-51.133	-68.675	-49.774	-43.651	-36.899	-30.776
P5WB	-49.997	-67.821	-49.021	-42.841	-36.128	-29.948
P5WC	-50.373	-67.287	-48.889	-42.748	-36.179	-30.038
P6WA	-61.765	-82.248	-61.673	-55.183	-45.347	-38.857
P6WB	-61.176	-81.758	-60.285			
P6WC	-60.353	-82.019	-60.135			
P6WD	-60.612	-80.993	-60.134			
P6WE	-60.382	-82.467	-59.607			

^a Raw interaction energies refer to energies not corrected for either ZPE or BSSE. ^b $\Delta E(\text{RHF/I})^1$: interaction energy at RHF/6-31G(d,p) optimized geometry. ^c $\Delta E(\text{MP2/I})^2$: interaction energy at MP2/6-31G(d,p) optimized geometry. ^d $\Delta E(\text{MP2/II})^3$: interaction energy at MP2/6-311++G(2d,2p)(6d,10f) optimized geometry. ^e $\Delta E_{\text{ZPE-corr}}$: ZPE-corrected interaction energy at MP2/6-311++G(2d,2p)(6d,10f) optimized geometry. ^f $\Delta E_{\text{BSSE-corr}}$: BSSE-corrected interaction energy at MP2/6-311++G(2d,2p)(6d,10f) optimized geometry. ^g $\Delta E_{\text{ZPE+BSSE}}$: Interaction energy corrected for ZPE and BSSE corrections at the MP2/II level optimized geometry. ^h We could locate an energetically different structure that is also a minimum on PES. However, it is almost similar to that of P4WD and hence is not repeated here.

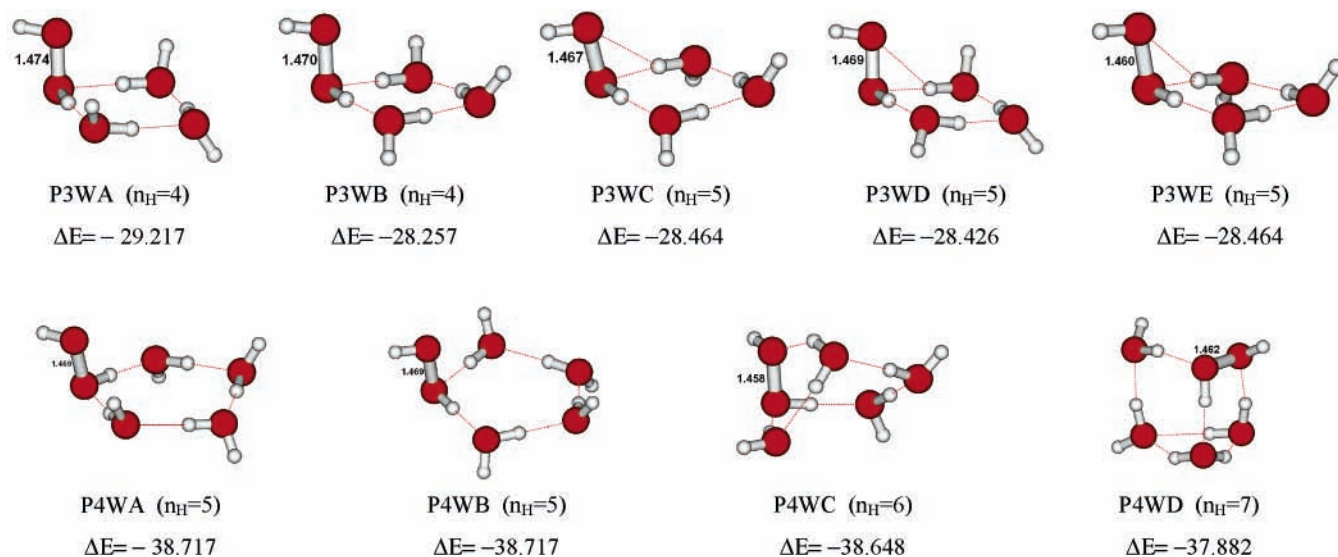


Figure 2. MP2/6-311++G(2d,2p) (6d,10f) optimized structures of H₂O₂⋯(H₂O)_n, n = 3 and 4 clusters, along with the number of hydrogen bonds (*n*_H), O–O distances and the corresponding interaction energies in kcal·mol⁻¹. All of the distances are given in angstroms. See the text for further details.

combination of a water dimer²² having binding cooperativity with a hydrogen peroxide molecule, by virtue of the H bonds. To obtain a fuller perspective of the molecular cooperativity and gauge the significance of the pairwise interactions among monomeric units within the clusters, we have performed many-body interaction-energy analysis by employing the MBAC computer code.²⁷ According to MBAC calculations, the H₂O⋯H₂O interaction in P2WA ($\Delta E = -4.899$ kcal·mol⁻¹) turns out to be slightly weaker than that in the water dimer (H₂O)₂, ($\Delta E = -5.289$ kcal·mol⁻¹). It should also be noted that the lowest energy structure reported herein (P2WA) is

energetically more favorable (by ~ 2.69 kcal·mol⁻¹ at the MP2/6-311++G(2d,2p) (6d,10f) level) than the one reported by Ju et al.²¹

Remarkably, for *n* = 3, all of the structures bear very close resemblance to water tetramers,²² with one of the hydrogen atoms in a H₂O unit getting appropriately converted into an OH group (cf. Figure 2). It should be noted that all of the structures lie within a narrow energy range of ~ 0.8 kcal·mol⁻¹ above the most favorable structure (P3WA). Also, it is observed that with increasing *n*, several energetically comparable structures emerge by flipping selected hydrogen atoms in a given structure, a

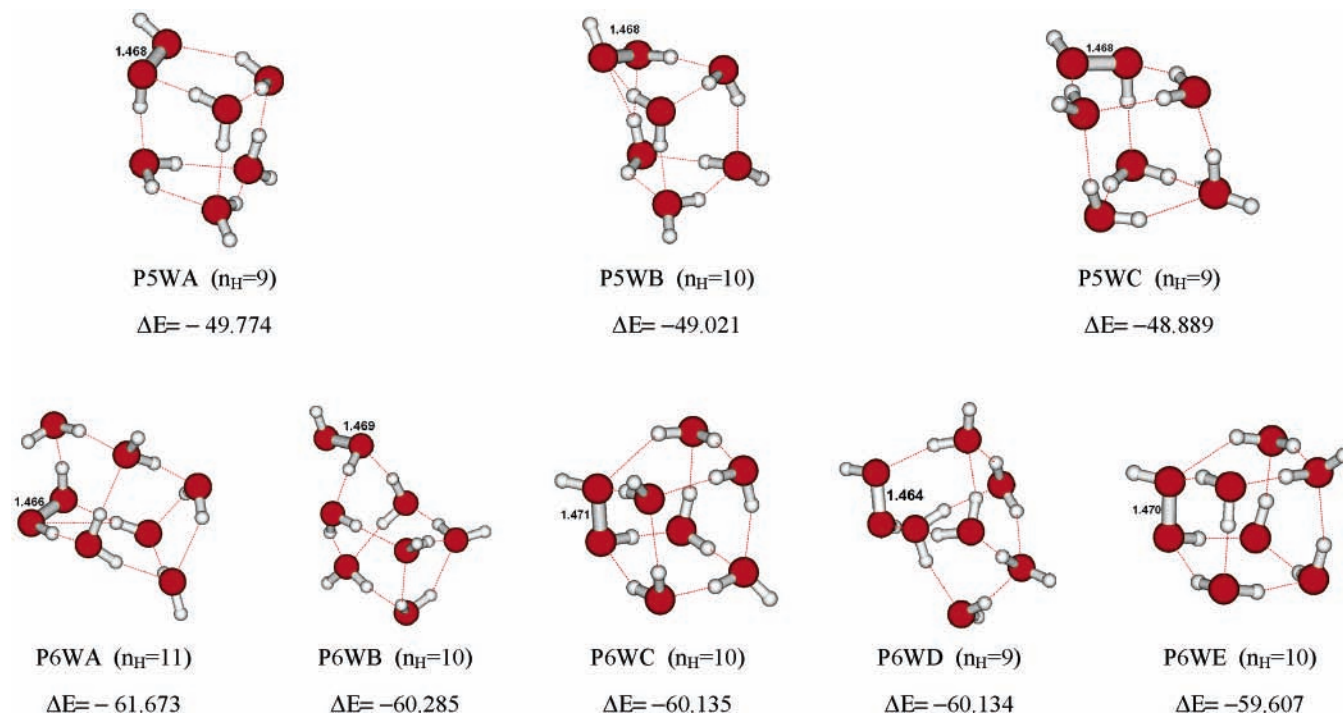


Figure 3. MP2/6-311++G(2d,2p) (6d,10f) optimized structures of $\text{H}_2\text{O}_2 \cdots (\text{H}_2\text{O})_n$, $n = 5$ and 6 clusters, along with the number of hydrogen bonds (n_H), O–O distances and the corresponding interaction energies in $\text{kcal}\cdot\text{mol}^{-1}$. All of the distances are given in angstroms. Refer to the text for further details.

TABLE 2:

A: Many-body interaction-energy analysis for the lowest-energy structures of $\text{H}_2\text{O}_2 \cdots (\text{H}_2\text{O})_n$ clusters at the MP2/6-311++G(2d,2p) (6d,10f) level^a

energy term	$n = 2$	$n = 3$	$n = 4$	$n = 5$	$n = 6$
2-body energy	-16.213 (-4.899)	-24.042 (-11.658)	-30.420 (-17.969)	-42.788 (-28.095)	-53.812 (-33.571)
3-body energy	1.940	-6.143	-8.487 (-3.278)	-7.662 (-4.429)	-9.750 (-2.405)
4-body energy			-1.173 (-0.229)	-1.260 (-0.594)	-1.534 (-0.183)
higher-body energy			0.074	0.244	0.096
E_R^b	0.001	0.969	1.434	1.690	3.327
ΔE	-18.148	-29.217	-38.717	-49.774	-61.673

B: A comparison of pairwise (viz., $\text{H}_2\text{O}_2 \cdots \text{H}_2\text{O}$ and $\text{H}_2\text{O} \cdots \text{H}_2\text{O}$) interaction energies from many-body interaction-energy analysis for the most favorable structures of $\text{H}_2\text{O}_2 \cdots (\text{H}_2\text{O})_n$ clusters at the MP2/6-311++G(2d,2p) (6d,10f) level^c

Cluster \downarrow Interactions \rightarrow	$E(\text{H}_2\text{O} \cdots \text{H}_2\text{O})$	$E(\text{H}_2\text{O}_2 \cdots \text{H}_2\text{O})$
$\text{H}_2\text{O} \cdots \text{H}_2\text{O}$ in $(\text{H}_2\text{O})_2$	-5.289	
$\text{H}_2\text{O}_2 \cdots \text{H}_2\text{O}$		-7.395
$\text{H}_2\text{O}_2 \cdots (\text{H}_2\text{O})_2$	-4.899	-6.578
$\text{H}_2\text{O}_2 \cdots (\text{H}_2\text{O})_3$	-5.016	-6.279
$\text{H}_2\text{O}_2 \cdots (\text{H}_2\text{O})_4$	-4.909	-5.888
$\text{H}_2\text{O}_2 \cdots (\text{H}_2\text{O})_5$	-5.007	-6.212
$\text{H}_2\text{O}_2 \cdots (\text{H}_2\text{O})_6$	-5.004	-6.179

^a The energy values are in $\text{kcal}\cdot\text{mol}^{-1}$. The values in the parentheses indicate the energy contribution to $\text{H}_2\text{O} \cdots \text{H}_2\text{O}$ interactions in the given molecular system. See text for details. ^b E_R = Relaxation energy. ^c The energy values are in the units of $\text{kcal}\cdot\text{mol}^{-1}$. See text for details. $E(\text{H}_2\text{O} \cdots \text{H}_2\text{O})$ and $E(\text{H}_2\text{O}_2 \cdots \text{H}_2\text{O})$ are the values obtained in the many-body analysis.

feature akin to the one observed by Maheshwary and co-workers²² for their exhaustive study on water clusters. The oxygen atoms in the present $n = 3$ clusters almost lie in a plane, and some of these clusters show the presence of multiple hydrogen bonding, a signature of the increased cooperativity resulting in forming a 3D structure. This observation holds well even for the clusters with $n = 4$. The four energetically favorable structures for $n = 4$ are portrayed in Figure 2, with the energies given in Table 1. Interestingly enough, the most favorable structures (P4WA and P4WB), despite being energetically degenerate, are structurally different as seen from the different

relative orientations of the H atoms in the H_2O molecules. Figure 2 also shows that with an increasing number of hydrogen bonds the clusters evince a remarkable resemblance to 3D clusters of water molecules,²² where, for the latter, the transformation from (almost) planar to 3D networks of clusters occurs especially for $n \geq 6$. To obtain energetically favorable structures for $n = 4-6$ we have scanned at least 30 structures at the RHF/6-31G-(d,p) level with the best 5 chosen for a follow-up at higher levels of theory. Once again, it is observed that these structures show a striking resemblance to the “cage” and “prism” form of $(\text{H}_2\text{O})_6$, water hexamer clusters.²²

TABLE 3:

A: Vibrational frequency analysis of the energetically most favorable H₂O₂···(H₂O)_n, n = 1–4, clusters at the MP2/6-311++G(2d,2p) (6d,10f) level^a

cluster	frequency, cm ⁻¹	intensity, KM·mol ⁻¹	assignment
H ₂ O ₂	915.8	0.8	O–O s
	1333.5	109.6	O–H b
	3819.0	19.2	O–H ss
	3819.4	67.9	O–H as
H ₂ O ₂ ···H ₂ O	1355.3, 1519.8	93.9, 39.2	O–H t
	1656.2	69.6	H–O–H b (W)
	3660.6	267.7	O–H s (P)+ (W)
	3809.5	67.4	O–H s (W)
	3815.4	38.1	O–H s (W)+ (P)
	3947.6	115.0	O–H as (W)
	H ₂ O ₂ ···(H ₂ O) ₂	1355.3, 1548.5	68.4, 39.0
1667.9, 1685.3		78.6, 17.5	H–O–H b (W)
3516.8, 3641.9		457.5, 444.9	O–H s (P) +(W)
3719.8		412.2	O–H ss (W)
3819.2		47.4	O–H s (P)
3933.3, 3933.8		174.6, 60.1	O–H as (W)
H ₂ O ₂ ···(H ₂ O) ₃		850.1	207.7
	1031.2, 1362.4, 1563.5	49.2, 82.6, 19.9	O–H t (P)
	1683.3, 1696.3	79.8, 57.9	H–O–H b (W)
	3353.0, 3517.1	682.7, 768.9	O–H s (P)+ (W)
	3572.1, 3639.1	813.8, 435.3	O–H ss (W)
	3818.7	43.7	O–H s (P)
	3923.2, 3924.3, 3929.2	98.6, 96.3, 84.5	O–H as (W)

B: Vibrational frequency analysis of the lowest-energy clusters of H₂O₂···(H₂O)_n, n = 5 and 6, at the MP2/6-311++G(2d,2p) (6d,10f) level

cluster	frequency, cm ⁻¹	intensity, KM·mol ⁻¹	assignment
H ₂ O ₂ ···(H ₂ O) ₄	911.5, 930.5	59.4, 118.5	O–O s (P)
	1041.3, 1370.9, 1544.6	37.0, 75.1, 38.9	O–H t (P)
	1685.1, 1697.5	41.1, 78.2	H–O–H b (W)
	3331.9, 3461.6, 3508.2	808.9, 1012.4, 1474.8	O–H s (W) + (P)
	3551.7, 3614.8	376.9, 403.7	O–H ss (W) + O–H (P)
	3816.7	41.4	O–H s (P)
	3922.3, 3926.4, 3927.8, 3930.0	89.1, 98.1, 84.5, 79.3	O–H as (W)
	H ₂ O ₂ ···(H ₂ O) ₅	903.6, 938.7	35.2, 62.9
1361.3, 1599.6		73.6, 23.7	O–H t (P)
1669.7, 1693.2,		117.7, 57.9,	H–O–H b (W)
1717.6		31.4	O–H b (W)+ O–H b (P)
1730.0, 1749.2		146.7, 28.6	H–O–H b (W)
3277.4		615.8	O–H s (W)
3363.8		1142.0	O–H s (P) + (W)
3556.6, 3630.7, 3725.0, 3733.7		367.8, 371.4, 135.5, 240.5	O–H ss (W)
3805.6		337.6	O–H as (W)
3821.7		62.7	O–H s (P)
H ₂ O ₂ ···(H ₂ O) ₆	3833.6, 3835.3, 3920.1, 3926.3	109.8, 355.9, 83.9, 104.7	O–H as (W)
	921.8, 931.6	63.4, 25.9	O–O s (P)
	1006.3, 1544.2	72.1, 66.3	O–H t (P)
	1666.2, 1689.4, 1695.6, 1699.6	143.8, 59.1, 31.7, 58.3	H–O–H b (W)
	1723.7, 1741.0	27.9, 54.9	H–O–H b (W)
	3325.1, 3415.7	753.4, 960.3	O–H s (P)+ (W)
	3498.6	827.7	O–H s (P)
	3614.2	331.7	O–H ss (W)
	3646.9, 3714.2	450.1, 198.4	O–H s (W) + (P-weak)
	3730.9	269.0	O–H s (W)
H ₂ O	3800.4, 3836.6, 3914.1, 3915.9	471.4, 233.2, 90.0, 83.6	O–H as (W)
	3919.8, 3926.4	111.3, 107.2	O–H as (W)
	1660.4	65.2	H–O–H b
	3862.0	9.8	O–H ss
	3983.1	73.3	O–H as

^a Legend: O–O s = O–O stretching, O–H t = O–H torsion, H–O–H b = H–O–H bending, O–H s = O–H stretch, O–H ss = O–H symmetric stretch, O–H as = O–H asymmetric stretch, (P) = vibrations corresponding to H₂O₂, (W) = vibrations corresponding to H₂O, (P) + (W) = contaminating (mixed) vibrations corresponding to H₂O₂ and H₂O. The intensity values are in the same order as that of frequencies. See text for details.

As opposed to the case of H₂O₂···(H₂O)_n, n = 1–4, where the majority of the clusters bear the water molecules (their oxygen atoms) in an almost planar form, for the present n = 5, deviation from planarity occurs, resulting in distorted cage-like patterns. Figure 3 depicts the three most favorable

H₂O₂···(H₂O)₅ clusters, namely, P5WA, P5WB, and P5WC, with the interaction energies of –49.774, –49.021, and –48.889 kcal·mol⁻¹, respectively. For n = 6, five of the most favorable clusters, namely, P6WA, P6WB, P6WC, P6WD, and P6WE, as shown further in Figure 3, where increased hydrogen bonding

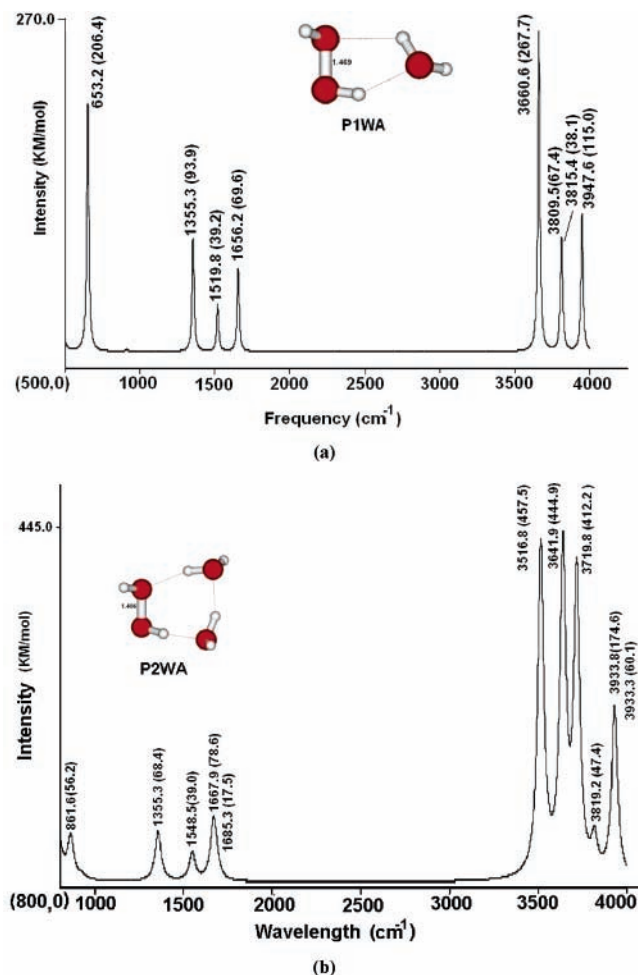


Figure 4. Simulated IR spectrum of $\text{H}_2\text{O}_2 \cdots (\text{H}_2\text{O})_n$, $n = 1$ and 2 clusters, respectively, namely, (a) P1WA and (b) P2WA computed at the MP2/6-311++G(2d,2p)(6d,10f) level of theory. All of the distances are given in angstroms. Please refer to the text for details.

is evident. The energetics of Table 2 brings out the fact that the ZPE-corrected interaction energies exhibit the same trend of relative stability. The best possible structure for $n = 6$ (P6WA) shows an energy jump of $-11.024 \text{ kcal}\cdot\text{mol}^{-1}$ over the best structure of $n = 5$, after addition of one H_2O . This particular stability can be traced back to the increase in the two-body energy contribution to the interaction energy of the P6WA structure, as borne out by many-body-interaction analysis (cf. Table 2). Interestingly again, the $\text{H}_2\text{O}_2 \cdots (\text{H}_2\text{O})_6$ clusters show cage-like patterns and similarity to $(\text{H}_2\text{O})_8$ clusters.²² The average number of hydrogen bonds for $n = 6$ ($n_{\text{H}} = 10$) exceeds that for $n = 5$ by unity. It may be observed that the overall trends in the energetics (cf. Table 1) at the RHF level are mimicked by the MP2 level of theory as well. Also, as is well-known^{22,29,31c} and has been reaffirmed recently by Rablen et al.,^{29a} a higher basis set or higher level of theory is accompanied by a decrease in the numerical value of the interaction energy. The present authors have also noted similar trends in their earlier studies.^{22,31c} However, the use of higher basis sets has been recommended in the literature for reducing the BSSE.³⁰ It is our observation that the use of a basis set such as 6-311++G-(2d,2p) (essentially of triple- ζ quality), indeed reduces the BSSE to a considerable extent ($\sim 8\%$ or less).²² Hence, we have employed a similar basis set, namely, 6-311++G(2d,2p)-(6d,10f), which is effective in reducing the BSSE (around 12%) of the interaction energy (ΔE). The reason for this increase in BSSE-correction values may be attributed to compactness of

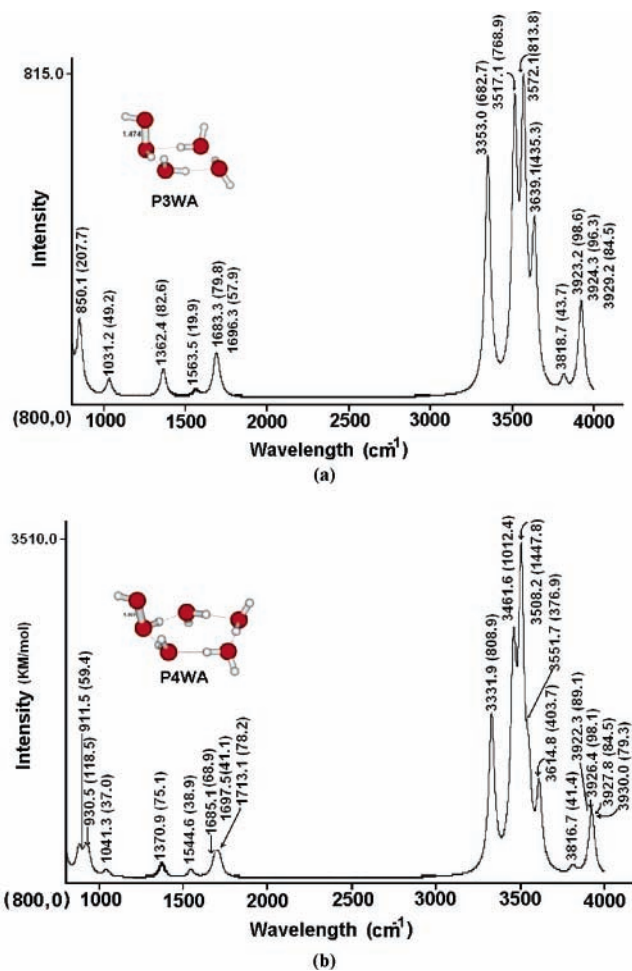


Figure 5. Simulated IR spectrum of $\text{H}_2\text{O}_2 \cdots (\text{H}_2\text{O})_n$, $n = 3$ and 4 clusters, respectively, namely, (a) P2WA and (b) P4WA computed at the MP2/6-311++G(2d,2p)(6d,10f) level of theory. All of the distances are given in angstroms. Please refer to the text for details.

the structures. Additional sample calculations performed at the MP2/aug-cc-pV5Z//MP2/6-311++G(2d,2p)(6d,10f) level for the $\text{H}_2\text{O}_2 \cdots \text{H}_2\text{O}$ (P1WA) and $\text{H}_2\text{O}_2 \cdots (\text{H}_2\text{O})_2$ (P2WA) complex bring the reduction in BSSE correction to only a marginal value, namely, 2.462 and 2.516, respectively, leading to an average percent BSSE correction that is $\sim 2.5\%$ of the interaction energy. Table 1 makes it evident that the application of BSSE and ZPE, individually or in conjunction, invariably lowers the interaction energy. It may be noted that inclusion of both BSSE and ZPE has been reported to give an overcorrection,^{31a,b,c} yet, the overall trends in the energetics are seen to remain, by and large, the same.

It is worth noting that with increasing number of H_2O molecules, the O—O bond elongation in H_2O_2 is only marginal, in contrast with the earlier results by Ju et al.²¹ However, a careful look at their results shows fluctuations in the O—O bond length.

Many-body interaction-energy analysis is summarized in Table 2. For all of the lowest energy structures of $\text{H}_2\text{O}_2 \cdots (\text{H}_2\text{O})_n$, $n = 2-6$, the two-body- and three-body interaction-energy terms dominate, contributing to more than 97% of the interaction energy, forming the attractive or stabilizing part of the interaction energy, whereas the four-body, the higher-body (>4), and the relaxation energies (E_{R}) form the repulsive part of the interaction. This observation is similar to the earlier observations of peroxide clusters by S. Kulkarni

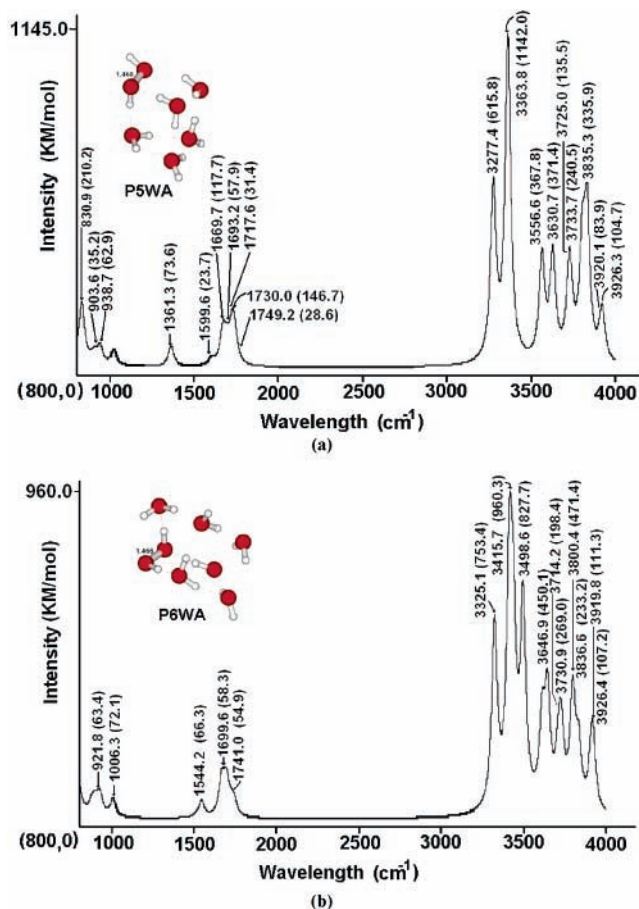


Figure 6. Simulated IR spectrum of H₂O₂⋯(H₂O)_n, n = 5 and 6 clusters, respectively, namely, (a) P5WA and (b) P6WA computed at the MP2/6-311++G(2d,2p)(6d,10f) level of theory. Please refer to the text for details. All of the distances are given in angstroms.

and co-workers,^{20a} of water clusters by Xantheas,^{20b} and of larger water and hydrated clusters reported by A. Kulkarni et al.²⁷

Vibrational Frequency Analysis. To investigate the effect of growth of H₂O₂⋯(H₂O)_n clusters on their spectral features, we have performed the vibrational frequency analysis at the MP2/6-311++G(2d,2p)(6d,10f) level, which for the case of n = 6 turned out to be computationally very demanding. Table 3 presents unscaled vibrational frequencies of the most stable H₂O₂⋯(H₂O)_n clusters along with their respective IR intensities. Figures 4–6 show the qualitative IR spectra *simulated* at the MP2/6-311++G(2d,2p)(6d,10f) level of theory. The Figures depicted here represent the simulated IR spectra for the energetically most favorable structures. The actual experimental spectra, however, will have a mixture of spectral features due to several energetically comparable conformers. It may be seen from Table 3 as well as from Figures 4–6 that the first vibrational mode of O–H torsional bending shows a shift in wavelength from 1355 to 1006 cm⁻¹ along with a decrease in the intensity, the latter depicted here in KM/mol. The other significant vibrational modes, namely, H–O–H bending and O–H stretching, with an increase in the number of water molecules, show a splitting of the vibrations into multiplets. For example, the symmetric stretching mode of O–H bonds in water for P1WA, appearing at 3815.4 cm⁻¹, shows splitting of its vibrational frequencies as doublet, doublet, triplet, triplet, and quartet for the number of water molecules (n) being 2, 3, 4, 5 and 6, respectively. This effect may be attributed to an

increase in asymmetry with successive addition of water molecules to the cluster that seems to (at least partially) lift the degeneracy.

A reference to Table 3 and Figures 4–6 brings out the fact that these vibrations show reasonable shifts to lower frequencies, indicating a weakening of the respective bonds involved in the mode of vibration. The bond-weakening effect is also shown by the relaxation energy (E_R) values coming from the many-body interaction-energy analysis (Table 2), which show a steady increase of cluster growth. Remarkably, we observe an appearance of O–O stretching vibrations (with reasonable intensity) in the case of H₂O₂⋯(H₂O)_n clusters, for n = 4–6.

IV. Conclusions

This article investigates the structure and energetics of H₂O₂⋯(H₂O)_n, n = 1–6, clusters at an ab initio level, the most sophisticated one employed being MP2/6-311++G(d,2p)(6d,10f). All of these clusters show a very close structural resemblance to the higher water clusters, namely, (H₂O)_{n+1} or (H₂O)_{n+2}. The smaller clusters (n ≤ 3) contain the water molecules in an almost planar fashion; larger clusters (n ≥ 4) show a cage-like structure akin to their corresponding water cluster counterparts. It is observed that clustering with addition of water molecules results in only a slight weakening of the O–O bond in the peroxide and increased asymmetry that is borne out by the many-body analysis that separately computes two-body to n-body interaction energies contributing to the total energy. Of these, the two-body and three-body interaction-energy contributions constitute a large and attractive part of the interaction energy (~97%), whereas the higher-order contributions (four-body and higher) constitute the repulsive portion. Increasing sophistication, by and large, maintains that the trends in the energetics are at all of the levels: the structures observed at the MP2/6-311++G(2d,2p)(6d,10f) level are qualitatively similar to those predicted at RHF/6-31G(d,p) level of theory. Hence, for these systems, even the RHF/6-31G(d,p) level can be regarded as a reliable level for an *initial* scanning of possible geometries and understanding the trends. The energy trends do not alter after inclusion of ZPE, although its inclusion results in a relative destabilizing of the ΔE values by ~25–31% of the respective uncorrected ΔE values. In the present case, the inclusion of BSSE-correction results in marginally destabilizing the ΔE values by ~12% of the respective uncorrected ΔE values. However, the inclusion of BSSE does not alter the trends in the energetics. Nevertheless, employment of a sophisticated basis set, aug-cc-pV5Z, to estimate the BSSE effect for the H₂O₂⋯H₂O (P1WA) and H₂O₂⋯(H₂O)₂ (P2WA) cluster gives the average percent BSSE correction as small as ~2.5% of the interaction energy.

A detailed study, on the lines of the present work, with a greater number of water molecules would be required for observing significant O–O elongation and discrete hydration of H₂O₂. The present study is expected to provide the initial pathways toward such an extension. This study, as well as a complementary investigation of hydration of two or more peroxide molecules is also underway.

Acknowledgment. A.D.K. is thankful to Dr. Shridhar P. Gejji (Department of Chemistry, University of Pune) for several useful discussions. R.K.P. gratefully acknowledges a Senior Group Associateship to the Abdus Salam International Center for Theoretical Physics, where a part of this problem was carried out.

References and Notes

- (1) Seinfeld, J. H.; Pandis, S. N. *Atmospheric Chemistry and Physics*; J. Wiley Interscience: New York, 1998; pp 249, 356.
- (2) Hoffmann, M. R.; Edwards, J. O. *J. Phys. Chem.* **1975**, *79*, 2096.
- (3) Peukett, S. A.; Jones, B. M. R.; Brice, K. A.; Eggleton, A. E. *Atmos. Environ.* **1979**, *13*, 123.
- (4) Martin, L. R.; Damschen, D. E. *Atmos. Environ.* **1981**, *15*, 1615.
- (5) Kunen, S. M.; Lazrus, A. L.; Kok, G. L.; Heikes, B. G. *J. Geophys. Res.* **1983**, *88*, 3671.
- (6) McArdle, J. V.; Hoffmann, M. R. *J. Phys. Chem.* **1983**, *87*, 5425.
- (7) Reeves, C. E.; Penkette, S. A. *Chem. Rev.* **2003**, *103*, 5199.
- (8) (a) Bell, G. H.; Davidson, J. N.; Emslie-Smith, D. *Textbook of Physiology and Biochemistry*, 7th ed; ELBS: London, 1968. (b) Fontecave, M.; Peirre, J. L. *Bull. Soc. Chim. Fr.* **1991**, *128*, 505. (c) Hoffmann, M.; Schleyer, R. R. *J. Am. Chem. Soc.* **1994**, *116*, 4947. (d) Hofmann-Sievert, R.; Castleman, A. W., Jr. *J. Phys. Chem.* **1984**, *88*, 3329.
- (9) Benassi, R.; Fiantri, L. G.; Tadde, F. *J. Org. Chem.* **1995**, *60*, 5855.
- (10) (a) Goebel, J.; Ault, B. S.; Del Bene, J. E. *J. Phys. Chem. A* **2000**, *104*, 2033. (b) Goebel, J.; Ault, B. S.; Del Bene, J. E. *J. Phys. Chem. A* **2001**, *105*, 6430.
- (11) (a) Goebel, J.; Ault, B. S.; Del Bene, J. E. *J. Phys. Chem. A* **2001**, *105*, 11365. (b) Goebel, J.; Antle, K. A.; Ault, B. S.; Del Bene, J. E. *J. Phys. Chem. A* **2002**, *106*, 6406.
- (12) Shi, Y.; Zhou, Z. *J. Mol. Struct.: THEOCHEM* **2004**, *674*, 113.
- (13) Beichert, P.; Schremes, O. *J. Phys. Chem. A* **1998**, *102*, 10540.
- (14) (a) Dobado, J. A.; Molina, J. M. *J. Phys. Chem. A* **1999**, *103*, 4755. (b) Dobado, J. A.; Molina, J. M.; Portal, D. *J. Phys. Chem. A* **1998**, *102*, 778.
- (15) (a) Dobado, J. A.; Molina, J. M.; Portal, D. *J. Mol. Struct.: THEOCHEM* **1998**, *433*, 181. (b) Daza, M. C.; Dobado, J. A.; Molina, J. M.; Villaveces, J. L. *J. Phys. Chem. A* **1999**, *103*, 4755.
- (16) Gonzalez, L.; Mo, O.; Yanez, M. *J. Comput. Chem.* **1997**, *18*, 1124.
- (17) (a) Engdahl, A.; Nelander, B.; Karlström, G. *J. Phys. Chem. A* **2001**, *105*, 8393. (b) Engdahl, A.; Nelander, B. *Phys. Chem. Chem. Phys.* **2000**, *2*, 3967.
- (18) Dobado, J. A.; Molina, J. M. *J. Phys. Chem.* **1994**, *98*, 1819.
- (19) Mo, O.; Yañez, M.; Elguero, R. *J. Chem. Phys. Lett.* **1994**, *45*, 219.
- (20) (a) Kulkarni, S. A.; Pathak, R. K.; Bartolotti, L. *J. Chem. Phys. Lett.* **2001**, *372*, 620. (b) Xantheas, S. S. *J. Chem. Phys.* **1994**, *100*, 7523.
- (21) Ju, X. H.; Xiao, J. J.; Xiao, H. M. *J. Mol. Struct.: THEOCHEM* **2003**, *626*, 231.
- (22) Maheshwary, S.; Patel, N.; Sathyamurthy, N.; Kulkarni, A. D.; Gadre, S. R. *J. Phys. Chem. A* **2001**, *105*, 10525.
- (23) Frisch, M. J.; Trucks, G. W.; Schlegel, H. B.; Scuseria, G. E.; Robb, M. A.; Cheeseman, J. R.; Zakrzewski, V. G.; Montgomery, J. A., Jr.; Stratmann, R. E.; Burant, J. C.; Dapprich, S.; Millam, J. M.; Daniels, A. D.; Kudin, K. N.; Strain, M. C.; Farkas, O.; Tomasi, J.; Barone, V.; Cossi, M.; Cammi, R.; Mennucci, B.; Pomelli, C.; Adamo, C.; Clifford, S.; Ochterski, J.; Petersson, G. A.; Ayala, P. Y.; Cui, Q.; Morokuma, K.; Malick, D. K.; Rabuck, A. D.; Raghavachari, K.; Foresman, J. B.; Cioslowski, J.; Ortiz, J. V.; Stefanov, B. B.; Liu, G.; Liashenko, A.; Piskorz, P.; Komaromi, I.; Gomperts, R.; Martin, R. L.; Fox, D. J.; Keith, T.; Al-Laham, M. A.; Peng, C. Y.; Nanayakkara, A.; Gonzalez, C.; Challacombe, M.; Gill, P. M. W.; Johnson, B. G.; Chen, W.; Wong, M. W.; Andres, J. L.; Head-Gordon, M.; Replogle, E. S.; Pople, J. A. *Gaussian 98*, revision A.7; Gaussian, Inc.: Pittsburgh, PA, 1998.
- (24) Schmidt, M. W.; Baldridge, K. K.; Boatz, J. A.; Elbert, S. T.; Gordon, M. S.; Jensen, J. H.; Koseki, S.; Matsunaga, N.; Nguyen, K. A.; Su, S. J.; Windus, T. L.; Dupuis, M.; Montgomery, J. A. *GAMESS. J. Comput. Chem.* **1993**, *14*, 1347.
- (25) Limaye, A. C.; Gadre, S. R. *Univis-2000: An Indigenously Developed Molecular Visualization Package. Curr. Sci. (India)* **2001**, *80*, 1296.
- (26) Schaftenaar, G.; Noordik, J. H. *MOLDEN: A pre- and post-processing program for molecular and electronic structures. J. Comput.-Aided Mol. Des.* **2000**, *14*, 123.
- (27) Kulkarni, A. D.; Ganesh, V.; Gadre, S. R. *J. Chem. Phys.* **2004**, *121*, 5043.
- (28) Elrod, M. J.; Saykally, R. *J. Chem. Rev.* **1994**, *94*, 1975.
- (29) (a) Rablen, P. R.; Lockman, J. W.; Jorgensen, W. L. *J. Phys. Chem. A* **1998**, *102*, 3782. (b) Kim, J.; Kim, K. S. *J. Chem. Phys.* **1998**, *109*, 5886. (c) Su, J. T.; Xu, X.; Goddard, W. A., III. *J. Phys. Chem. A* **2004**, *108*, 10518.
- (30) Scheiner, S. *Hydrogen Bond*; Oxford University Press: New York, 1997.
- (31) (a) Turi, L.; Dannenberg, J. J. *J. Phys. Chem.* **1995**, *99*, 639. (b) Wong, N.-B.; Cheung, Y.-S.; Wu, D. Y.; Ren, Y.; Wang, X.; Tian, A. M.; Li, W.-K. *J. Mol. Struct.* **2000**, *507*, 153. (c) Sundararajan, K.; Sankaran, K.; Viswanathan, K. S.; Kulkarni, A. D.; Gadre, S. R. *J. Phys. Chem. A* **2002**, *106*, 1504.